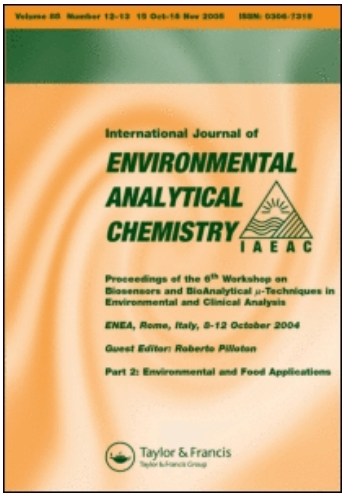

International Journal of Environmental Analytical Chemistry
Publication details, including instructions for authors and subscription information:
http://www.informaworld.com/smpp/title~content=t713640455

Fabrication and chemical surface modification of nanoporous silicon for biosensing applications

Shalini Singh[ab]; Shailesh N. Sharma[a]; S. M. Shivaprasad[a]; Mohan Lal[a]; Mukhtar A. Khan[b]
[a] Electronic Materials Division, National Physical Laboratory, New Delhi, India [b] Faculty of Life Science, Aligarh Muslim University, Aligarh, India

To cite this Article Singh, Shalini , Sharma, Shailesh N. , Shivaprasad, S. M. , Lal, Mohan and Khan, Mukhtar A.(2009) 'Fabrication and chemical surface modification of nanoporous silicon for biosensing applications', International Journal of Environmental Analytical Chemistry, 89: 3, 141 — 152
To link to this Article: DOI: 10.1080/03067310802331832
URL: http://dx.doi.org/10.1080/03067310802331832

Intern. J. Environ. Anal. Chem.
Vol. 89, No. 3, 15 March 2009, 141–152

Taylor & Francis
Taylor & Francis Group

Fabrication and chemical surface modification of nanoporous silicon for biosensing applications

Shalini Singh[ab], Shailesh N. Sharma[a]*, Govind[a], S.M. Shivaprasad[a], Mohan Lal[a] and Mukhtar A. Khan[b]

[a]*Electronic Materials Division, National Physical Laboratory, New Delhi, India;* [b]*Faculty of Life Science, Aligarh Muslim University, Aligarh, India*

(*Received 8 February 2008; final version received 8 July 2008*)

In this work, porous silicon (PS) films with varied porosity (68–82%) were formed on the *p*-type, boron-doped silicon wafer (100) by the electrochemical anodisation in an aqueous hydrofluoric acid and isopropyl alcohol solution at different current densities (I_d) ranging from 20–70 mA cm^{-2}, respectively. Biofunctionalisation of the PS surface was carried out by chemically modifying the surface of PS by the deposition of 3-aminopropyltriethoxysilane thermally leading to high density of amine groups covering the PS surface. This further promotes the immobilisation of immunoglobulin (human IgG and goat anti-human IgG binding) on to the PS surface. Formation of nanostructured PS and the attachment of antibody–antigen to its surface were characterised using photoluminescence (PL), Fourier transform infrared spectroscopy and X-ray photoelectron spectroscopy techniques, respectively. The possibility of using these structures as biosensors has been explored based on the significant changes in the PL spectra before and after exposing the PS optical structures to biomolecules. These experimental results open the possibility of developing optical biosensors based on the variation of the PL position of the PL spectra of PS-based devices.

Keywords: porous silicon; immunoglobin; biosensors; APTS

1. Introduction

The biosensor technology of porous silicon (PS) has received much attention because: (i) the fabrication of the sensor can be integrated with the well-established silicon microfabrication technology and hence the sensor can be easily characterised with electrical measurement, (ii) the significantly increased surface interaction area can enhance the detection signal, in either fluorescence or electrical measurements, (iii) the characteristic photoluminescence (PL) of PS makes it a special functional material for biosensing, (iv) the mesoporous nanostructures of PS can reflect light and thus coupled biomolecules can be sensed by optical reflectivity [1–4]. Thus PS-based biosensors can be of significant use in medical, chemical, biotechnology, etc [5]. For the biomedical applications of PS, biomolecules have to be first immobilised on its surface through functional groups deposited on it. The common approach is to create a covalent bond between the PS surface and the biomolecules which specifically recognise the target analytes [5,6]. The reliability of a biosensor strongly depends on the functionalisation

*Corresponding author. Email: shailesh@mail.nplindia.ernet.in

ISSN 0306–7319 print/ISSN 1029–0397 online

DOI: 10.1080/03067310802331832
http://www.informaworld.com

process depending on its fastness, simplicity, homogeneity and its repeatability [7]. It is well known that after anodisation, the fresh silicon surface is predominately hydride-terminated which is quite reactive and sensitive to oxidation [7]. Thus, to increase the surface stability of PS, there is a need to functionalise the surface of PS by a suitable precursor.

In this article, we report the formation of nanostructured PS on boron-doped *p*-type silicon wafer (100) by electrochemical anodisation using aqueous hydrofluoric acid and isopropyl alcohol solution at different current densities of 20 and 50 mA cm^{-2}, respectively. Here, the organic functionalisation of the PS surfaces was performed by 3-aminopropyltriethoxysilane (APTS) treatment thermally. The APTS is one of the most common precursors, which by following the appropriate process, can leave amine groups (NH_2) available for reaction with either a cross-linking agent or directly with a molecule and thus provides a reliable interface between biomolecules and a wide range of materials [8]. The optical behaviour of PS was determined before and after the biofunctionalisation process and after immobilisation of biomolecules.

2. Experimental

Boron-doped *p*-type Si monocrystalline wafers of (100) orientation, 0.5 Ω cm resistivity and 400 μm thickness were used for preparing PS. PS samples were formed by electrochemical etching using Si as the anode and Pt as the counter electrode in an acid-resistant Teflon container. A thin aluminium layer was evaporated on the back of the wafers and sintered to form an ohmic contact. The anodisation was carried out at different current densities $I_d \sim 20$ and 50 mA cm^{-2}, respectively for 30 min, in a solution of H_2O : HF : IPA (1 : 1 : 2). After etching, the samples were rinsed with propanol and dried under a stream of dry high-purity nitrogen prior to use. In the present work, nanostructured PS surface was biofunctionalised by the deposition of APTS thermally at 100°C for about 4–5 h [4]. The silane APTS is one of the most common precursors, which by following the appropriate process, can leave amine groups (NH_2) available for reaction with either a cross-linking agent or directly with a molecule [4]. The samples were thoroughly rinsed with propanol and dried under stream of pure nitrogen. The sample after APTS attachment was characterised by photoluminescence (PL), Fourier transform infrared spectroscopy (FTIR) and X-ray photoelectron spectroscopy (XPS). The functionalised PS was immersed into a solution of glutaraldehyde (2.5%) i.e. 2.5 mL of glutaraldehyde in 97.5 mL of DI water (v/v) (pH 7), which was used as a cross linker. The wafers were kept in the solution for 1 h at room temperature. It was important to rinse successively with DI water in order to remove all excess of glutaraldehyde. The antibody (human IgG) (5 μg mL^{-1} in acetic/acetate buffers, pH 5) was immobilised on treated PS surface. Then 0.1% bovine serum albumin (BSA), a blocking agent was incorporated which also increase hydrophilicity. The substrates were cleaned with 0.05% Tween 20 in phosphate buffered saline (PBS), then they were put in contact with antigen (goat anti-human IgG) for 1 h and then rinsed with buffer (0.05% Tween 20 in PBS) solution and finally the substrates were rinsed with DI water.

The PL was measured using a home assembled system consisting of a two-stage monochromator, a photomultiplier tube (PMT) with a lock-in amplifier for PL detection and an Ar^+ ion laser operating at 488 nm and 5 mW (corresponding to 0.125 W cm^{-2}) power for excitation. XPS measurements were performed in an ultra-high vacuum

chamber (PHI 1257) with a base pressure of $\sim 4 \times 10^{-10}$ torr. The XPS spectrometer is equipped with a high-resolution hemispherical electron analyzer (279.4 mm diameter with 25 meV resolution) and a Mg (K_α) ($h\nu = 1253.6$ eV) X-ray excitation source.

3. Results and discussion

The porosity of PS films as estimated from gravimetric measurements [9] varied from 65–75% corresponding to I_d ranging from 20 to 70 mA cm^{-2}, respectively.

Typical PL curves for PS films formed at different current densities I_d on unpolished substrates corresponding to electrolyte $H_2O:HF:IPA$ (1:1:2) are shown in Figure 1(A)(a–d). As evident from Figure 1(A)(b), the absolute PL intensity is higher for PS formed at $I_d \sim 50$ mA cm^{-2} with PL band centred $\lambda_{PL} \sim 660$ nm. For $I_d \sim 60$ mA cm^{-2}, PL peak shifts towards red ($\lambda_{PL} \sim 690$ nm) with decrease in PL intensity (Figure 1A(c)). However, at further higher $I_d \sim 70$ mA cm^{-2}, the PL intensity decreases drastically with PL peak significantly blue-shifted ($\lambda_{PL} \sim 609$ nm) (Figure 1A(d)). At this I_d, the films are powdery, non-adherent to the substrate and have a peeling-off tendency. At a lower $I_d \sim 20$ mA cm^{-2}, the PL intensity of PS film is low and PL intensity profile ($\lambda_{PL} \sim 611$ nm) (Figure 1A(a)) is quite similar to that obtained for $I_d \sim 70$ mA cm^{-2}. An increase in current density or an increase in PS porosity always led to a blue-shift of the PL spectra. However, in our study, the surprising difference is the reverse dependence of the PL peak position on the PS porosity. With increase in current density from 20 to 60 mA cm^{-2}, the subsequent shift of the PL spectra towards red end of the spectrum could be due to the effect of the oxide-related species on the surface of PS as observed earlier [10]. This could be due to the breaking of Si–Si bonds with concomitant decrease in Si-skeleton size and formation of Si–O bonds [10]. The interface region being passivated by oxygen all the same, there was only a slight decrease in the PL intensity in the case of higher porosity sample for $I_d \sim 60$ mA cm^{-2}. However, at further higher $I_d \sim 70$ mA cm^{-2}, due to excessive etching of the Si-skeleton, the PL intensity decreases significantly. As shown in Figure 1(A)(e and f), upon APTS treatment, the PS film corresponding to $I_d \sim 20$ and 50 mA cm^{-2} shows a PL quenching with considerable decrease in PL intensity. Since the absolute PL intensity for fresh PS at $I_d \sim 50$ mA cm^{-2} is higher as compared to $I_d \sim 20$ mA cm^{-2} as evident from Figure 1(A)(a and b), similar trend is obtained for their corresponding APTS-treated films as well (Figure 1A(e and f)). The fact that APTS is a charge acceptor provides an indication that the quenching of PL most probably occurs via a charge transfer mechanism. This irreversible quenching can also be attributed to a chemical modification of the PS sample that generates non-radiative surface traps resulting in decrease in PL intensity upon APTS attachment [11]. Moreover, concomitant shift of the PL peak position towards lower wavelength (blue-shift) upon APTS treatment particularly for $I_d \sim 50$ mA cm^{-2} indicates breaking of Si–Si bonds which causes reduction in Si-skeleton dimensions. The blue-shift particularly for $I_d \sim 50$ mA cm^{-2} upon APTS treatment is evident from the right inset of Figure 1(A). Here, upon APTS treatment, the peak position has shifted to ~609 nm from the untreated one at ~650 nm (Figure 1A(b)) with considerable decrease in PL intensity.

Visual observation shows that the PS films at $I_d \sim 50$ mA cm^{-2} appear more uniform and strong as compared to PS films formed at lower and higher current densities ($I_d \sim 20$ and 70 mA cm^{-2}), respectively. Thus, $I_d \sim 50$ mA cm^{-2} is the optimised I_d where a higher PL intensity is obtained and thus silanisation experiments (APTS treatment) and

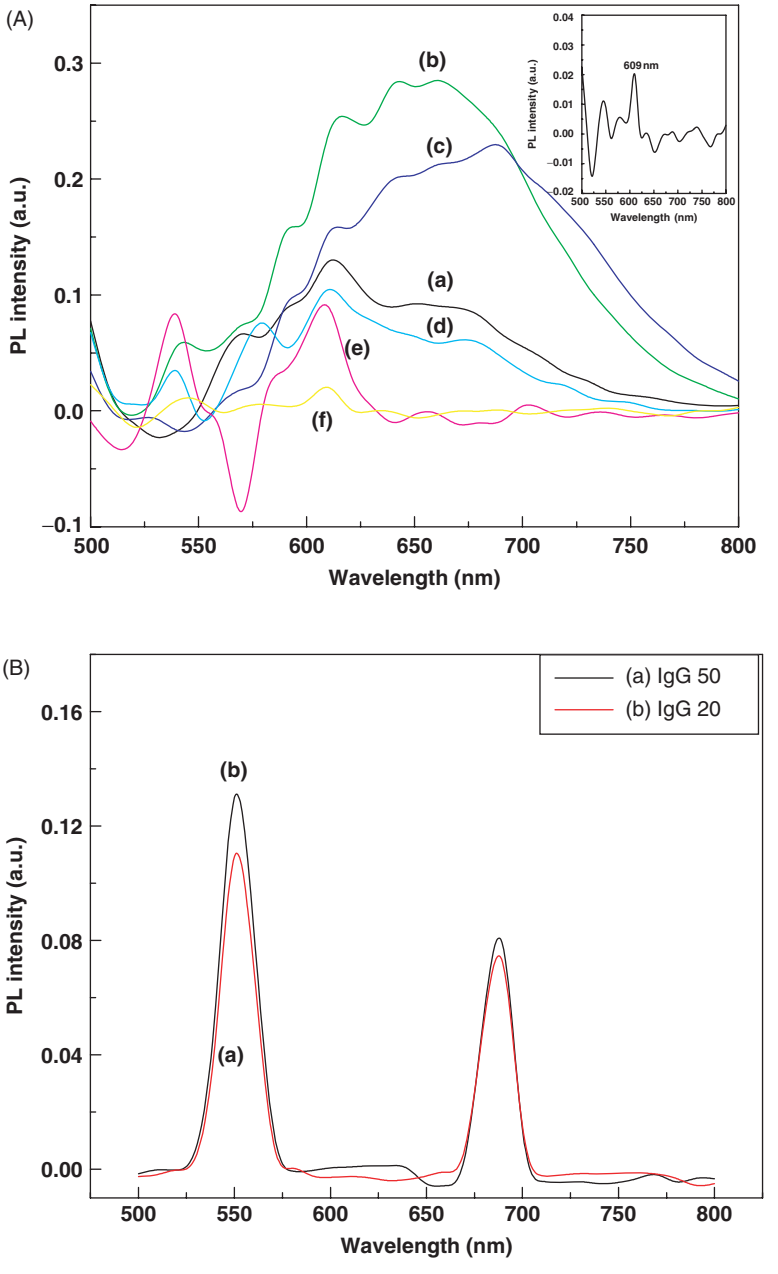

Figure 1. (A) PL spectra of fresh and APTS-treated PS prepared at different I_d; (a) Fresh PS; $I_d \sim 20\,mA\,cm^{-2}$; (b) Fresh PS; $I_d \sim 50\,mA\ cm^{-2}$; (c) Fresh PS; $I_d \sim 60\,mA\,cm^{-2}$; (d) Fresh PS; $I_d \sim 70\,mA\,cm^{-2}$; (e) and (f) after APTS treatment of PS prepared at $I_d \sim 20$ and $50\,mA\,cm^{-2}$; the inset shows the magnified version of PL spectrum of APTS-treated PS ($I_d \sim 50\,mA\,cm^{-2}$) and (B) upon IgG attachment; $I_d \sim 20\,mA\,cm^{-2}$ (curve a) and $I_d \sim 50\,mA\,cm^{-2}$ (curve b).

subsequent biomolecule (immunoglobulin) attachment is carried out. PS films with initial higher PL intensity are required so that effective charge transfer resulting in PL quenching upon silanisation can be carried out effectively. The results are compared with that for low porosity PS film at $I_d \sim 20\,mA\,cm^{-2}$.

Figure 1(B)(a and b) shows PL spectra of APTS-treated PS films upon attachment of IgG protein for $I_d \sim 20$ and $50\,mA\,cm^{-2}$, respectively. From Figure 1(B), it can be inferred that PL increases appreciably for APTS-treated PS film upon attachment of IgG protein as compared to APTS-treated PS films alone. The two new PL peaks at 550 and 690 nm implies the role of surface species ($-NH_2$) groups in modifying the luminescence characteristics of APTS-treated PS film. The PL doublets can be associated with Si and surface species ($-NH_2$) or to surface species alone. As such, the two band PL structure would require a bimodal distribution of nanoscale unit sizes in PS, however, this phenomenon can be explained by quantum confinement/luminescent centres QCLC model which indicates the presence of two kinds of luminescent centres (LC) in SiO_x layers covering the nanoscale silicon units in PS [12]. In the QCLC model, the electrons and holes inside the nanoscale (NS) units are excited by incident light and diffuse to the surfaces of the NS units, there they recombine to emit the visible light through the luminescent centres adsorbed on the surfaces of the NS units or tunnel separately to electron or hole excitation states of LCs in SiO_x layers which cover the NS units, then relax to ground states and recombine to emit visible light. If there are one or two kinds of LCs, correspondingly, the PL spectrum of PS has a single peak or double peak structure. The similarity in the PL spectra for APTS-treated PS films upon IgG attachment for both $I_d \sim 20$ and $50\,mA\,cm^{-2}$ indicates that this procedure leads to reproducible results for a wide range of surface conditions of the biofuctionalised PS. This result might open the way to the development of optical biosensors based on the change of the PL spectrum of PS before and after the immobilisation of different biomolecules.

Figure 2(A and B) shows SEM images of PS films corresponding to $I_d = 20$ and $50\,mA\,cm^{-2}$. As shown in Figure 2, with increase in I_d from 20 to $50\,mA\,cm^{-2}$, the pore size increases from 30–40 nm to 50–60 nm, respectively. Increase in current density not only increases the pore size but pore density as well evident from the SEM images (Figure 2).

Figure 3(A and B) (curves a and b) shows the IR transmittance spectra of fresh PS and APTS-treated PS corresponding to $I_d \sim 20$ and $50\,mA\,cm^{-2}$, respectively. From Figure 3(A)(a), the fresh PS film ($I_d \sim 20\,mA\,cm^{-2}$) exhibit Si–H related modes at $\sim 2104\,cm^{-1}$ due to Si–H stretching mode, $895\,cm^{-1}$ due to $Si–H_2$ scissors or $Si–H_3$ symmetric or anti-symmetric deformation, $640\,cm^{-1}$ due to Si–H wagging [10,13,14]. It is important to note that as prepared PS corresponding to lower $I_d \sim 20\,mA\,cm^{-2}$ has a broad band at $\sim 1250\,cm^{-1}$ corresponding to Si–O–Si stretching modes [10,13]. Similarly, for $I_d \sim 50\,mA\,cm^{-2}$, the FTIR spectra (Figure 3B(a)) shows Si–H related modes at; 2105, 875 and $622\,cm^{-1}$ corresponding to Si–H stretching, $Si–H_2$ scissors or $Si–H_3$ symmetric or anti-symmetric deformation and Si–H wagging modes, respectively and a band at $1240\,cm^{-1}$ corresponds to Si–O–Si stretching mode [10,13,14]. For $I_d \sim 20\,mA\,cm^{-2}$, upon treatment of PS film with APTS, the Si–H related modes at ~ 640, 895 and $2104\,cm^{-1}$ as observed in fresh PS film completely vanishes (Figure 3A(a and b)). Similar trend is obtained for higher $I_d \sim 50\,mA\,cm^{-2}$ (Figure 3B(b)). This observation implies a hydrosilylation reaction that consumes Si–H bonds (preferentially SiH_2 and SiH_3) rather than cleaving Si–Si bonds alone as reported for the thermal reaction of alcohols [15] and Grignard [16] and alkyl lithium [17] reagents with PS. The FTIR of the APTS-treated

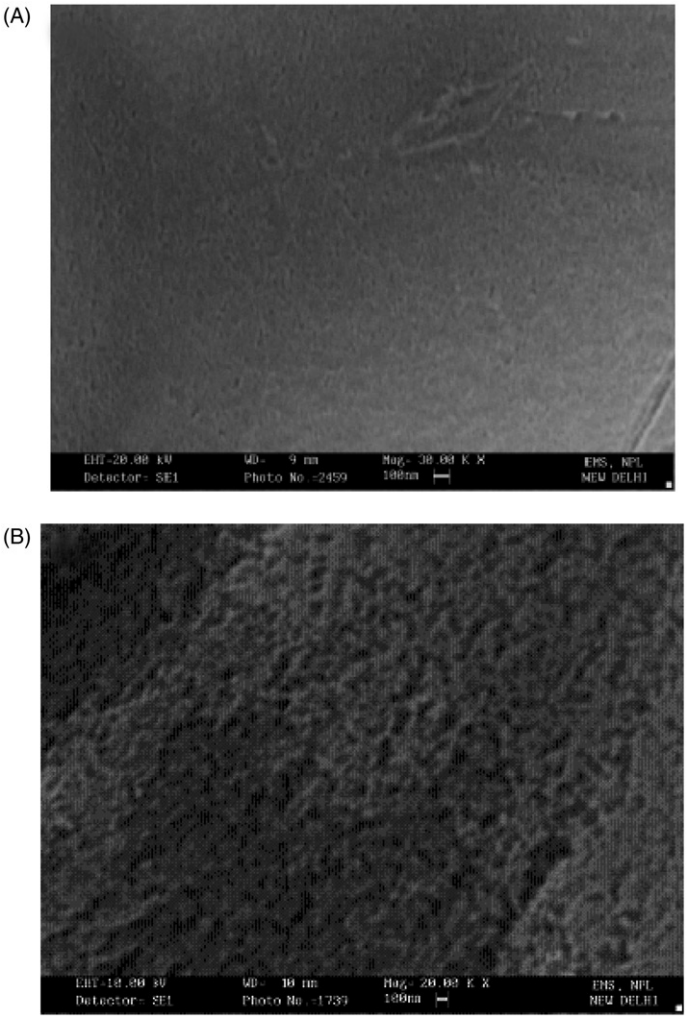

Figure 2. SEM images of fresh PS prepared at different I_d; (A) $I_d \sim 20\,mA\,cm^{-2}$, (B) $I_d \sim 50\,mA\,cm^{-2}$.

PS film ($I_d \sim 20\,mA\,cm^{-2}$) as shown in Figure 3(A)(b) shows presence of new peaks viz. $\sim$2965 cm^{-1} corresponding to vibrational bands of CH_x (x = 1–3) [2,18] and $\sim$1680 cm^{-1} corresponding to bending modes of NH_2 [2,18]. The corresponding peaks for $I_d \sim 50\,mA\,cm^{-2}$ are at 2980 and 1720 cm^{-1}, respectively. The absence of Si–H bonds on the surface of APTS-treated PS film for both $I_d \sim 20$ and $50\,mA\,cm^{-2}$, implies efficient coverage of amines ($-NH_2$) groups on PS surface. This result is in contrast with other reports where steric hindrance was observed upon introduction of the organic molecules thus resulting in insufficient coverage on the PS surface [19].

In order to identify the species responsible for the change in PL characteristics of PS, FTIR studies of PS films upon IgG attachment were carried out. Figure 3(C)(a and b) shows the FTIR spectrum of APTS-treated PS surface upon immunoglobulin attachment for $I_d \sim 20$ and $50\,mA\,cm^{-2}$, respectively. The presence of amine and carbon-related

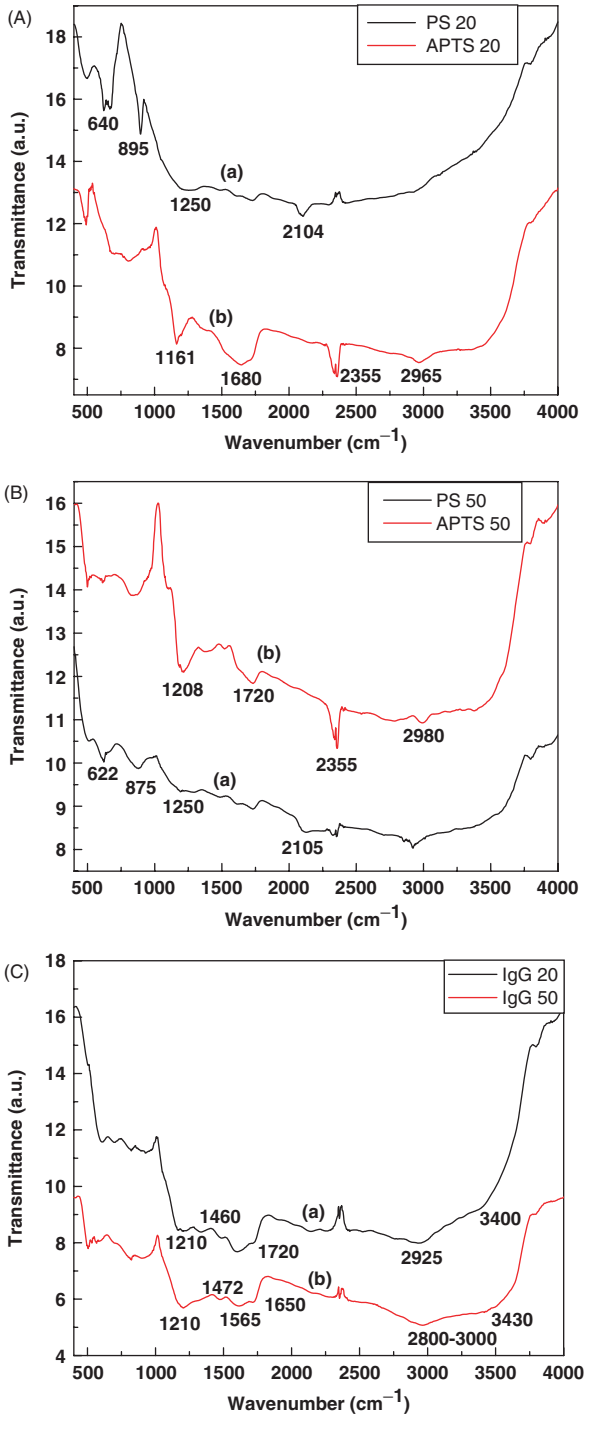

Figure 3. FTIR transmittance spectra of fresh PS (A), APTS-treated (B) and IgG attached PS (C) prepared at different $I_d \sim 20\,mA\,cm^{-2}$ (curve a) and $50\,mA\,cm^{-2}$ (curve b), respectively.

groups are evident by the presence of the following IR modes: 1210 cm^{-1} (SiO–Si stretching), 1472 cm^{-1}(CH_x (x = 1–3) deformation mode), 1650 cm^{-1} (C = O strecht of amide I), 1565 cm^{-1} (C–N strecht and C–N–H in plane bend in the strecht-bend mode of amide II bond), 2800–3000 cm^{-1} (carbonyl group C=O of amino acids), 2925–2962 cm^{-1} (CH_x stretching mode), 3400–3430 cm^{-1} (NH-stretching) [4,20–22]. From Figure 3(C), the presence of IgG is clearly evident from the changes in IR spectra of APTS-treated PS films (Figure 3B) which shows successful immobilisation of protein on the silanised surface of PS films.

Figure 4(A)(a–d) shows the Si(2p) core-level XPS spectra for fresh PS and APTS-treated PS corresponding to $I_d \sim 20$ and 50 mA cm^{-2}, respectively. From Figure 4(A),

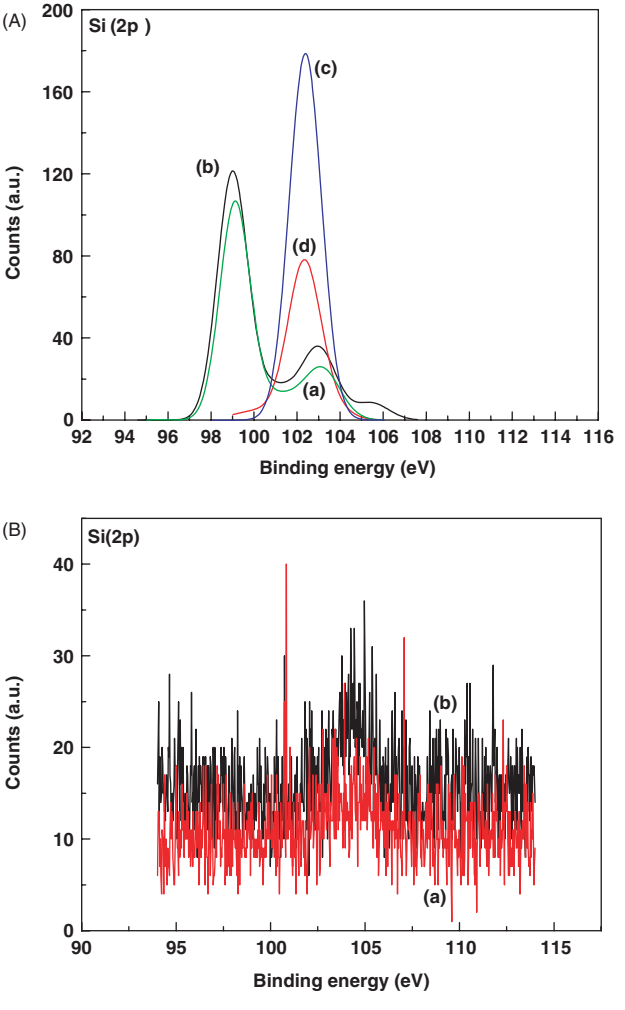

Figure 4. XPS Si (2p) core-level spectra of fresh PS and APTS-treated PS prepared at different I_d; (A) (a) and (b) fresh PS, $I_d \sim 20$ mA cm^{-2} and 50 mA cm^{-2}; (c) and (d) the corresponding APTS-treated PS; (B) upon immunoglobulin (Human IgG and Goat anti-human IgG) attachment; (a) $I_d \sim 20$ mA cm^{-2} and (b) $I_d \sim 50$ mA cm^{-2}.

curves (a and b) for fresh PS for both $I_d \sim 20$ and 50 mA cm^{-2}, the Si(2p) core level spectra shows the doublet at ~99.0 and 103 eV which indicates that Si exists in two different environments; pure Si and oxidised Si [23,24]. However, APTS-treated PS shows Si(2p) singlet peak at ~102.3 eV (Figure 4A(c and d)) which indicates that for thermally treated PS sample for silanisation, the entire PS surface is silanised with no evidence of any pure single crystal Si peak.

Figure 4(B)(curves a and b) shows the Si(2p) XPS spectra of APTS-treated PS films correspond to $I_d \sim 20$ and 50 mA cm^{-2} upon immunoglobulin (human IgG and goat anti-human IgG binding) attachment. Since the IgG molecules can be immobilised onto the surface of APTS-treated PS only than on fresh PS, because of the presence of reactive NH_2 groups on treated sample as compared to the fresh one. However, upon IgG attachment onto APTS-treated PS films ($I_d \sim 20$ and 50 mA cm^{-2}), the Si(2p) peak almost disappeared and showed a weak signal at 103.4 eV (Figure 4B(a and b). The disappearance of the Si(2p) peak suggests that the thickness of the immunoglobulin layer and the APTS layer must have exceeded the escape depth of Si(2p) electron and is a proof of protein adsorption. However, from Figure 4(A and B), the singlet XPS peak at ~103 eV associated with Si(2p) core-level for APTS-treated PS and upon immunoglobulin attachment corresponding to both $I_d \sim 20$ and 50 mA cm^{-2} can be assigned to SiO_2 formed during APTS decomposition and later deposition [23] as also observed from PL results as well. The attenuation of the Si(2p) XPS signal upon immunoglobulin attachment further throws light that $-NH_2$ surface species modifies the PL characteristics of PS films.

Figure 5(A)(a–f) shows the C(1s) core-level XPS spectra for fresh PS, APTS-treated PS and upon IgG attachment corresponding to $I_d \sim 20$ and 50 mA cm^{-2}, respectively. Here the fresh PS films exhibits lower C content as compared to APTS-treated PS films which can be attributed to an increase in C– and N-like species upon silanisation for APTS-treated films (Figure 5A(a–d)). However, from Figure 5(A)(c and d), the high C XPS peak intensity for low porosity sample ($I_d \sim 20$ mA cm^{-2}) as compared to higher porosity PS film ($I_d \sim 50$ mA cm^{-2}) upon APTS treatment could possibly due to the atmospheric carbon contamination. When immunoglobulin (human IgG and goat anti-human IgG binding) are immobilised onto APTS-treated PS film, the C(1s) peak intensity increases more so for $I_d \sim 50$ mA cm^{-2} (Figure 5A(e and f)). The enhancement of the carbon content was due to the immobilisation of the protein which is significant for higher porosity PS film ($I_d \sim 50$ mA cm^{-2}) due to its vast surface area as compared to the corresponding lower porosity film ($I_d \sim 20$ mA cm^{-2}).

In the case of N(1s) core level XPS spectra (Figure 5B(a–d)), the peak position at ~399.0 eV for APTS-treated PS films for both $I_d \sim 20$ and 50 mA cm^{-2} and upon immunoglobulin attachment clearly shows the presence of $-NH_2$ species [24,25]. The absence of higher binding energy component here implies absence of any decomposition product of the APTS precursor. However, increment in N XPS signal upon IgG attachment is appreciable for higher porosity ($I_d \sim 50$ mA cm^{-2}) as compared to the corresponding lower porosity film ($I_d \sim 20$ mA cm^{-2}) possibly owing to higher rate of adsorption for the former as compared to the later. The increase in the width of the C(1s) XPS core-level spectrum with subsequent development of extra peak at 287.6 eV (C–N species) (Figure 5B(e and f)) and disappearance of Si(2p) XPS signal (Figure 4B(a and b)) upon IgG attachment is a proof of protein adsorption [26].

From O(1s) core-level spectra for lower porosity PS film upon APTS-treatment corresponding to $I_d \sim 20$ mA cm^{-2}, there is a remarkable enhancement in O-signal at ~531.7 eV [22] as compared to the corresponding fresh PS film (Figure 5C(a and c)). This

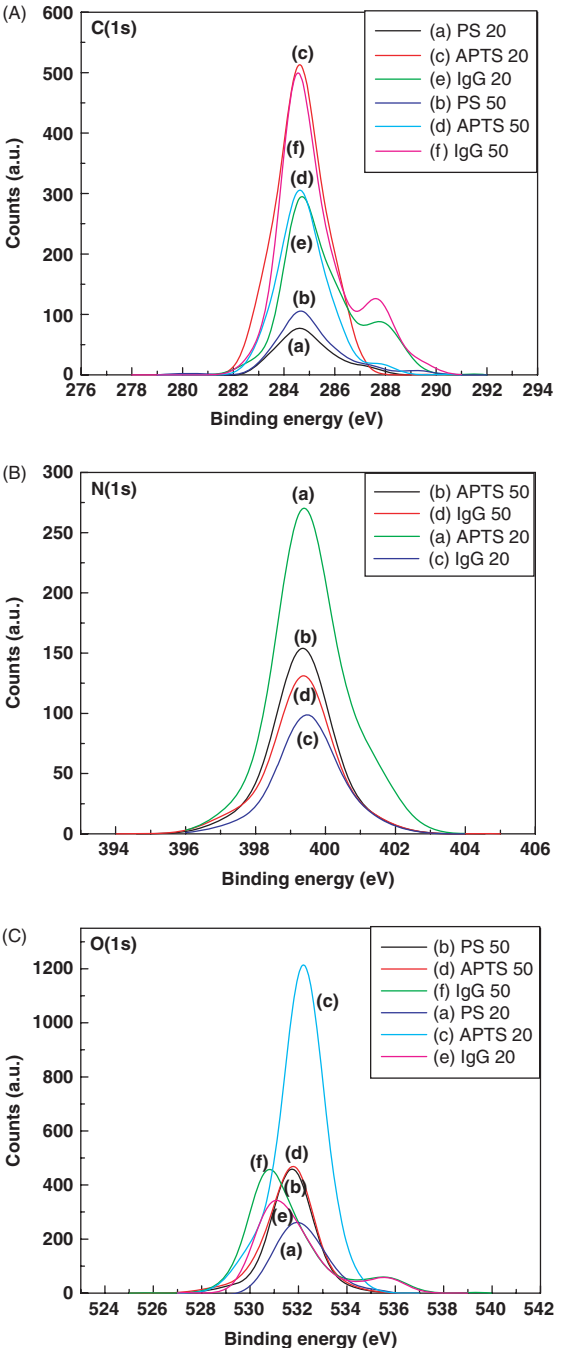

Figure 5. XPS core-level spectra of PS prepared at different I_d; (A) C(1s); (a) and (b) fresh PS, $I_d = 20$ and $50\,mA\,cm^{-2}$; (c) and (d) APTS-treated PS, $I_d = 20$ and $50\,mA\,cm^{-2}$; (e) and (f) the corresponding spectra upon immunoglobulin attachment, (B) N(1s); (a) and (b) APTS-treated PS, $I_d = 20$ and $50\,mA\,cm^{-2}$; (c) and (d) the corresponding spectra upon immunoglobulin attachment, (C) O(1s); (a) and (b) fresh PS, $I_d = 20$ and $50\,mA\,cm^{-2}$; (c) and (d) APTS-treated PS, $I_d = 20$ and $50\,mA\,cm^{-2}$; (e) and (f) the corresponding spectra upon immunoglobulin attachment.

is in contrast to higher porosity films ($I_d \sim 50\,mA\,cm^{-2}$), where the XPS spectra at ~530.7 eV of both fresh PS and upon APTS-treatment are almost similar as there is no discernible change (Figure 5C(b and d)). The shift of XPS O(1s) peak towards higher binding energy for low porosity PS film ($I_d \sim 20\,mA\,cm^{-2}$) as compared to that for $I_d \sim 50\,mA\,cm^{-2}$ upon APTS treatment again illustrates the fact that hydrosilylation of lower porosity PS film ($I_d \sim 20\,mA\,cm^{-2}$) involves oxidation as also documented by PL and FTIR studies as well. Thus, the results of XPS proved conclusively that the immunoglobulin was site-directly immobilised onto the APTS-treated PS surface.

4. Conclusions

In this work, we have fabricated PS films with varied porosity (68–82%) and pore-size (30–60 nm) formed at different I_d (20–70 $mA\,cm^{-2}$) for a fixed anodisation time of 30 min for its possible application as optical biosensors. Since the covalent attachment of specific biomolecules on the semiconductor surface is required for the realisation of biosensors based on molecular recognition, therefore, organic molecule APTS having an amine terminal was chosen to provide links for further functionalisation. The chemical APTS treatment facilitates the immobilisation of biomolecules immunoglobulin (human IgG and goat anti-human IgG binding) on to the functionalised PS surface as elucidated from PL, FTIR and XPS studies. The successful detection of antigen (goat anti-human IgG) and antibody binding on to the PS surface leads to significant PL changes which indicates that the functionalised nanoporous silicon can act as optical biosensing platform which is inexpensive and safe. Moreover, the large surface area of these nanoporous Si films particularly at $I_d \sim 50\,mA\,cm^{-2}$ makes them suitable candidates for high-throughput applications of optical biosensors.

Acknowledgements

We thank Director NPL for the encouragement to perform this work. Shalini Singh gratefully acknowledges CSIR (New Delhi) for SRF fellowship.

References

[1] H. Ouyang, C.C. Striemer, and P.M. Fauchet, Appl. Phys. Lett. **88**, 163108 (2006).
[2] L. De Stefano, L. Moretti, I. Rendina, A.M. Rossi, and S. Tundo, Appl. Opt. **43**, 167 (2004).
[3] L. De Stefano, L. Moretti, A.M. Rossi, M. Rocchia, A. Lamberti, O. Longo, P. Arcari, and I. Rendina, IEEE Trans. Nanotech. **3**, 49 (2004).
[4] O. Meskini, A. Abdelghani, A. Tlili, R. Mgaieth, N. Jaffrezic-Renault, and C. Martelet, Talanta **71**, 1430 (2007).
[5] L. Mongo, G. Vasapollo, M.R. Guascito, and C. Malitesta, Anal. Bioanal. Chem. **385**, 146 (2006).
[6] M.P. Stewart and J.M. Buriak, Adv. Mater. **12**, 859 (2000).
[7] L. De Stefano, L. Rotiroti, I. Rea, L. Moretti, G. Di Francia, E. Massera, A. Lamberti, P. Arcari, C. Sanges, and I. Rendina, J. Opt. A: Pure Appl. Opt. **8**, S 540 (2006).
[8] D.C. Tessier, S. Boughaba, M. Arbour, P. Roos, and G. Pan, Sensor. Actuat. B **120**, 220 (2006).
[9] O. Bisi, S. Ossicini, and L. Pavesi, Surf. Sci. Rep. **38**, 1 (2000).
[10] S.N. Sharma, R. Banerjee, and A.K. Barua, Curr. Appl. Phys. **3**, 269 (2003).

[11] S.E. Letant, B.R. Hart, S.R. Kane, M.Z. Hadi, S.J. Shields, and J.G. Reynolds, Adv. Mater. **16**, 689 (2004).
[12] S.N. Sharma, G. Bhagavannarayana, U. Kumar, R. Debnath, and S. Chandra Mohan, Physica E **36**, 65 (2007).
[13] S.N. Sharma, G. Bhagavannarayana, R.K. Sharma, and S.T. Lakshmikumar, Mat. Sci. Eng. B **127**, 255 (2006).
[14] S.N. Sharma, R. Banerjee, D. Das, S. Chattopadhyay, and A.K. Barua, Appl. Surf. Sci. **182**, 333 (2001).
[15] V.M. Dubin, F. Ozanam, and J.-N. Chazalviel, Thin Solid Films **255**, 87 (1995).
[16] N.Y. Kim and P.E. Laibinis, J. Am. Chem. Soc. **119**, 2297 (1997).
[17] N.Y. Kim and P.E. Laibinis, J. Am. Chem. Soc. **120**, 4516 (1998).
[18] J.H. Song and M.J. Sailor, J. Am. Chem. Soc. **120**, 2376 (1998).
[19] B. Xia, S.J. Xiao, D.J. Guo, J. Wang, J. Chao, H.B. Liu, J. Pei, Y.Q. Chen, Y.C. Tang, and J.N. Liu, J. Mater. Chem. **16**, 570 (2006).
[20] M. Arroyo-Hernandez, R.J. Martin-Palma, V. Torres-Costa, and J.M. Martinez Duart, J. Non-Cryst. Sol. **352**, 2457 (2006).
[21] V.K.S. Hsiao, J.R. Waldeisen, Y. Zheng, P.F. Lloyd, T.J. Bunning, and T.J. Huang, J. Mater. Chem. **17**, 4896 (2007).
[22] J. Blümel, J. Am. Chem. Soc. **117**, 2112 (1995).
[23] M.A. Hernandez, R.J.M. Palma, J.P. Rigueiro, J.P. Garcia-Ruiz, J.L. Garcia-Fierro, and J.M.M. Duart, Mat. Sci. Eng. C **23**, 697 (2003).
[24] T.V. Torchinskaya, N.E. Korsunskaya, L. Yu.Khomenkova, B.R. Dhumaev, and S.M. Prokes, Thin Solid Films **381**, 88 (2001).
[25] Y. Wang, S. Han, A.L. Briseno, R.J.G. Sanedrin, and F. Zhou, J. Mater. Chem. **14**, 3488 (2004).
[26] S. Sharma, R.W. Johnson, and T.A. Desai, Biosens. Bioelectron. **20**, 227 (2004).